Generalized description of the nonlinear optical force in laser trapping of dielectric nanoparticles

Anita Devi[1] and Arijit K. De[2,*]

[1]*Department of Physical Sciences, Indian Institute of Science Education and Research (IISER) Mohali, Knowledge City, Sector 81, SAS Nagar, Punjab 140306, India*

[2]*Department of Chemical Sciences, Indian Institute of Science Education and Research (IISER) Mohali, Knowledge City, Sector 81, SAS Nagar, Punjab 140306, India*

(Received 30 June 2020; accepted 9 October 2020; published 16 December 2020)

A general description to estimate optical trapping efficiencies for dielectric nanoparticles using dipole approximation is presented including the effect of optical nonlinearity. We show how optical nonlinearity can be harnessed to trap particles having a refractive index less than that of the surrounding medium. We also discuss optical trapping efficiencies of particles made of metamaterials of negative refractive indices. These results are promising in having wide-ranging applications in photonics science and technology.

DOI: 10.1103/PhysRevResearch.2.043378

I. INTRODUCTION

A laser tweezer is a tool used to both exert and measure miniscule force acting on small objects with sizes ranging from a micron down to a nanometer. After Ashkin and coworkers invented this technique in 1986 [1], which led to the Nobel Prize in Physics in 2018, it has been extensively used in several fields of natural science and technology [2–5]. For stable optical trapping of dielectric nanoparticles [5], a long-standing challenge is posed by the low polarizability volume as well as the erratic Brownian motion associated with these particles. To circumvent this, the common rule of thumb is to use very high laser power. However, such a high power may result in laser-induced heating effects, which is detrimental to the viability of live specimens and may eventually lead to irreversible specimen damage (laser-induced ablation). Therefore, it is essential to use an optimal laser power before experimentation. Fortunately, recent theoretical [6,7] as well as experimental [8] results on optical trapping of dielectric nanoparticles revealed that indeed there exists an optimal laser power corresponding to the most stable optical trap (refuting the widely accepted rule of thumb mentioned earlier) which results from a delicate balance between gradient and scattering forces and further fine-tuned by third-order optical nonlinearity, i.e., the optical Kerr effect (OKE). Although a noticeable effect of optical nonlinearity is expected to be observed at elevated laser power under conventional continuous-wave (CW) excitation, the same can be achieved at low average power under ultrashort pulsed excitation owing to its gigantic peak power. Note that a pulsed excitation leads to repetitive instantaneous momentum transfer [9], which also allows the system to thermally relax during the period between consecutive pulses (dead time) so that laser-induced heating effects are minimized. Extending our recent work [10], we focus on the origin of this optimal power; we theoretically show how OKE modulates the relative refractive index (of the particle to that of the surrounding medium) leading to controlled optical manipulation of dielectric nanoparticles. This work also provides a way to understand the need of antireflection coating for trapping of nanoparticles made of high refractive index materials [11,12] and trapping efficiencies of metamaterials with negative refractive indices [13].

II. GENERAL METHODOLOGY

In the dipole limit, the force expressions along axial directions can be written as [14]

$$F_{\text{scatter}}(r,\ z) = \frac{n^w k^4}{6\pi c}\,(4\pi a^3 M)^2 \left(\frac{2P}{\pi w_0^2}\right) \frac{1}{1+(2\tilde{z})^2} e^{-\frac{2\tilde{r}^2}{1+(2\tilde{z})^2}}, \tag{1}$$

$$F_{\text{gradient}}(r,\ z) = -\frac{n^w}{2c}\,4\pi a^3 M \left(\frac{2P}{\pi w_0^2}\right) \frac{8\tilde{z}/\left(k w_0^2\right)}{1+(2\tilde{z})^2} \left[1-\frac{2\tilde{r}^2}{1+(2\tilde{z})^2}\right] \frac{1}{1+(2\tilde{z})^2} e^{-\frac{2\tilde{r}^2}{1+(2\tilde{z})^2}}, \tag{2}$$

where $\omega_0 = 0.82 \times \lambda/NA$ is the spot size for the Gaussian beam profile and λ is the wavelength of the trapping beam and NA is the numerical aperture of the objective. $P = P_{\text{avg/peak}}$ is the average/peak power for the CW/pulsed excitation, a is the radius of the particle, $M = \left(\frac{m^2-1}{m^2+2}\right)$, $m = \frac{n^p}{n^w}$ is the relative refractive index (RI) of the particle (n^p) to the medium, water (n^w), and $\tilde{z} = \frac{z}{\pi\omega_0^2}$ and $\tilde{r} = \frac{r}{\omega_0}$ are reduced axial and radial coordinates, respectively. In the above equation, the polarizability (α) is highlighted in cyan, and the spatial coordinate-dependent part in gray. A detailed step-by-step description of the theoretical formulation of the final expression for force and potential is given in Sec. S1 in the

*Corresponding author: akde@iisermohali.ac.in

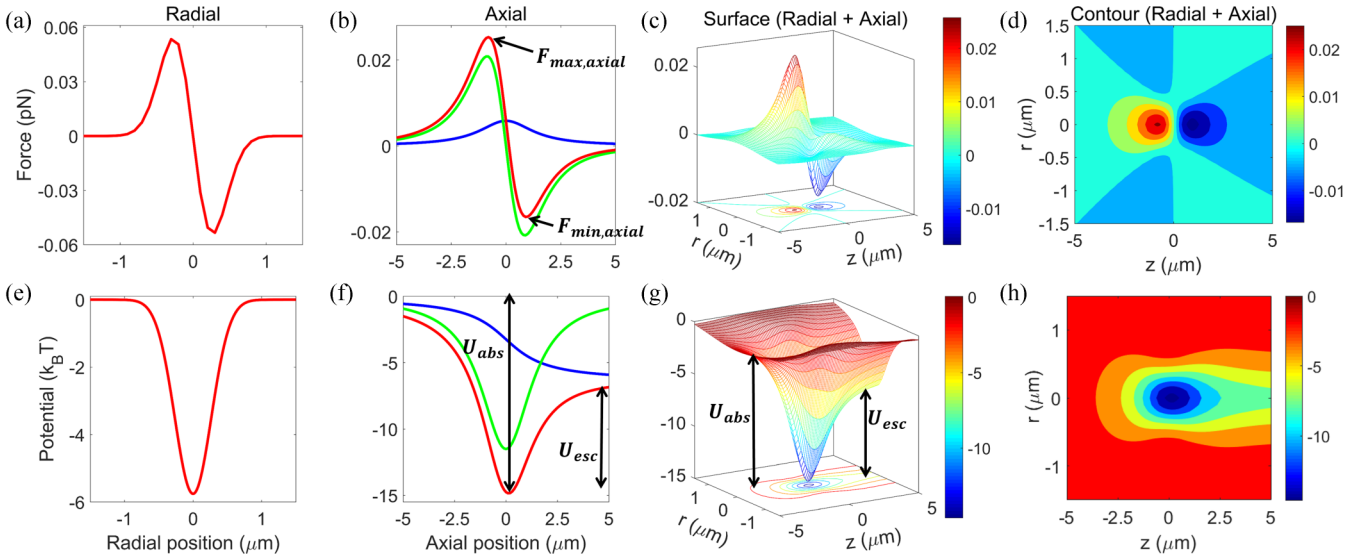

FIG. 1. Plots of trapping (a) radial force ($z = 0$), (b) axial force ($r = 0$), (c) surface force, (d) contour force, (e) radial potential ($z = 0$), (f) axial potential ($r = 0$), (g) surface potential, and (h) contour potential for 40 nm particle size under CW excitation. Color: green/blue curve corresponds to gradient/scattering force/potential along the axial direction, and red curve corresponds to total force/potential along both the axial and radial directions.

Supplemental Material (SM) [15]. The two equivalent methods to incorporate optical nonlinearity are rigorously derived in Secs. S1.1 and S1.2 in the SM [15]. In a numerical simulation, we have used the second method in which nonlinearity is incorporated in a phenomenological way:

$$n^w = n_0^w \quad \text{and} \quad n^p = n_0^p (\text{ CW excitation}), \tag{3a}$$

$$n^w \approx n_0^w \quad \text{and} \quad n^p = n_0^p + n_2^p \times I_{\text{peak}}(r, z) \text{ (pulsed excitation)}, \tag{3b}$$

where, $n_0^{w/p}$ is the linear refractive of the medium/particle, n_2^p is the second-order nonlinear RI of the particle, and $I_{\text{peak}}(r, z)$ is the peak intensity of a focused Gaussian beam under pulsed excitation. All parameters used in the simulation are listed in Table S1 in the SM [15]. Unless explicitly mentioned, we have chosen 100 mW average power and NA = 1.4 under both CW and pulsed excitation; the particle size corresponds to the radius of the particle.

III. RESULTS AND DISCUSSION

Figure 1 shows trapping force/potential curves for 40 nm polystyrene nanoparticles under CW excitation, where $F_{\text{max, axial}}$ and $F_{\text{min, axial}}$ represent the maximum and minimum of trapping force (marked by arrows), U_{abs} represents the absolute depth of the potential well, and U_{esc}, called the escape potential [6], is the potential barrier along the direction of light propagation.

From Eqs. (1) and (2), it can be seen that $M = (\frac{m^2-1}{m^2+2})$ is the crucial quantity to determine the nature of force; for example, $m < 1 \Leftrightarrow M < 1$ results in reversing the nature of gradient force from attractive to repulsive. However, irrespective of the m value, the nature of the scattering force remains the same because the scattering force varies as M^2. At $m = \pm 1$, both scattering and gradient forces vanish [as marked by the vertical green line in Fig. 2(a)] exerting no net force acting on the particle. Along the radial direction, only the gradient force acts; therefore, the value of m solely controls the nature of the force (attractive or repulsive). However, along the axial direction, the nature of the total force cannot be judged from the value of m alone because it is contributed by both gradient and scattering forces, which vary differently with m, as shown in Fig. 2(a). Beyond a certain threshold, M approaches a limiting value of 1 (because $m^2 - 1 \approx m^2$ and $m^2 + 2 \approx m^2$ when $m \gg 1$) irrespective of particle sizes, as shown in Fig. 2(b); the value of $\alpha = 4\pi a^3 M$ also reaches a limiting value (that depends on particle size). Under CW excitation, m is a constant quantity and independent of P_{avg}, ω_0, $\tilde{r}$, and $\tilde{z}$; therefore, change in any of these parameters does not change the nature of the force. Figures 2(c) and 2(d) show the trapping force along both the axial and radial directions for the different relative RI. For $m < 1$, $m = 1$, and $m > 1$, the particle experiences a repulsive force, zero force, and an attractive force, respectively. In the repulsive regime, the particle experiences an outward force that pushes it away from the trap. In the attractive regime, the particle experiences an inward force which pulls it towards the trap. This is also reflected in the potential curves [Figs. 2(e) and 2(f)]. Quite interestingly, a sudden change in the force/potential is observed from repulsive to attractive with a slight change in the relative RI. In order to trap the particle, the force must be attractive, and $F_{\text{max,axial}} > 0$ and $F_{\text{min,axial}} < 0$ are the required conditions. For a high relative RI, $F_{\text{max,axial}} > 0$ and $F_{\text{min,axial}} > 0$, and in this case, the force/potential becomes unbound, as shown in Figs. 2(g) and 2(h). In this regime, the trap is destabilized due to the dominance of scattering forces, so particles cannot be trapped. Similar behavior is observed for metamaterials (of negative m [13]) as well. Thus, depending on the value of the relative RI, the nature of forces/potentials is broadly categorized into three regimes: repulsive, attractive, and unbound. A detailed discussion of $F_{\text{max,axial}}$ and $F_{\text{min,axial}}$

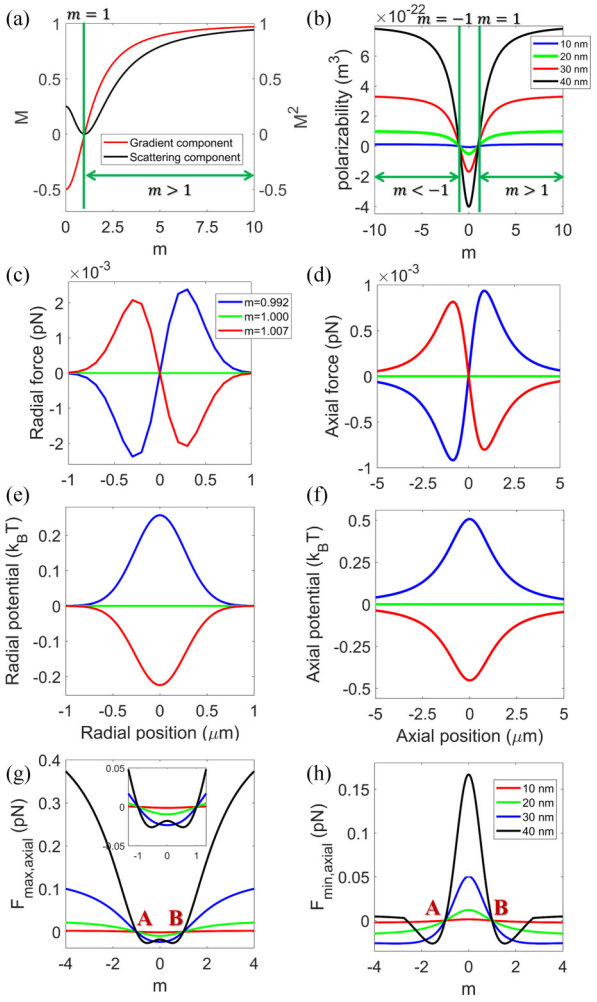

FIG. 2. Plots of (a) variation of M (gradient component) and M^2 (scattering component) against m and (b) polarizability against m. Plots of trapping force along the (c) radial and (d) axial directions and corresponding potential along the (e) radial and (f) axial directions. The plot of trapping force (g) maxima and (h) minima (shown in Fig. 1) against the relative RI for different particle sizes under CW excitation.

for different values of a, NA, and P_{avg} is given in Sec. S2.1 of the SM [15].

Under pulsed excitation, the relative RI is $\frac{n_0^p + n_2^p \times I_{\text{peak}}(r,z)}{n_0^w} = m + 4.44 \times 10^{-17} \times I_{\text{peak}}(r,z)$; here nonlinear RI of the medium can be ignored since it does not contribute significantly [6].

Figure 3 shows the trapping force/potential curves for 40 nm polystyrene nanoparticles under pulsed excitation, and a significant change in magnitude and nature of the force/potential curve is observed under similar conditions as compared to CW excitation (Fig. 1). Quite interestingly, under pulsed excitation, the nature of the force/potential is attractive for the m value 0.992, 1.000, and 1.007 [Figs. 4(a)–4(d)], whereas, under CW excitation, it shows the repulsive to attractive nature of the force/potential under similar conditions [Figs. 2(c)–2(f)]. A small change in the m (near $m = 1$) value does not significantly change the stability of the trap under pulsed excitation. This is because at 100 mW the average power nonlinearity contributes significantly, which results in a positive value of m. However, at very low average power (1 mW), where the contribution of nonlinearity is not significant, this transition behavior (repulsive to attractive) is present. Under pulsed excitation, the transition happens smoothly with relative RI because of nonlinearity, which we term the *intermediate regime*, whereas under CW excitation, this transition is abrupt. In this intermediate regime, the particle experiences both attractive and repulsive forces, and the stability of the trap depends upon their relative magnitudes. The regime of the relative RI changes with power, as shown in Fig. 4(e). The minima of M^2 shifts towards lower values of m with increasing average power. However, the range of the relative RI for which the force is repulsive or intermediate or attractive does not change with changing particle size, as shown in Fig. 4(f). An interesting feature is that for $m > 0.564$, the force/potential is always attractive, for $-0.301 < m < 0.564$, the force/potential shows an intermediate regime, and for $-1.353 < m < -0.301$, the force/potential is repulsive. This range changes with changing average power and NA, as shown in Figs. 4(g)

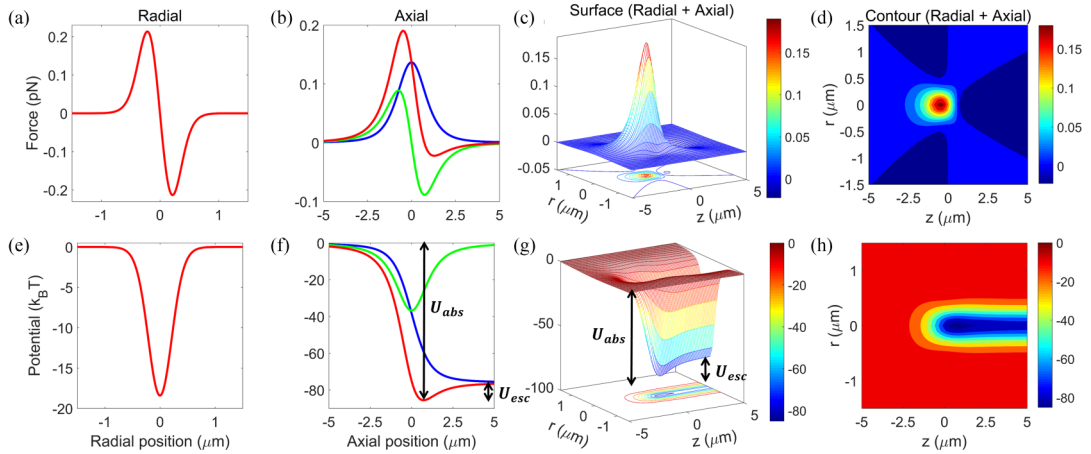

FIG. 3. Plots of trapping (a) radial force ($z = 0$), (b) axial force ($r = 0$), (c) surface force, (d) contour force, (e) radial potential ($z = 0$), (f) axial potential ($r = 0$), (g) surface potential, and (h) contour potential for 40 nm particle size under pulsed excitation. Color: green/blue curve corresponds to gradient/scattering force/potential along the axial direction, and red curve corresponds to total force /potential along both the axial and radial directions.

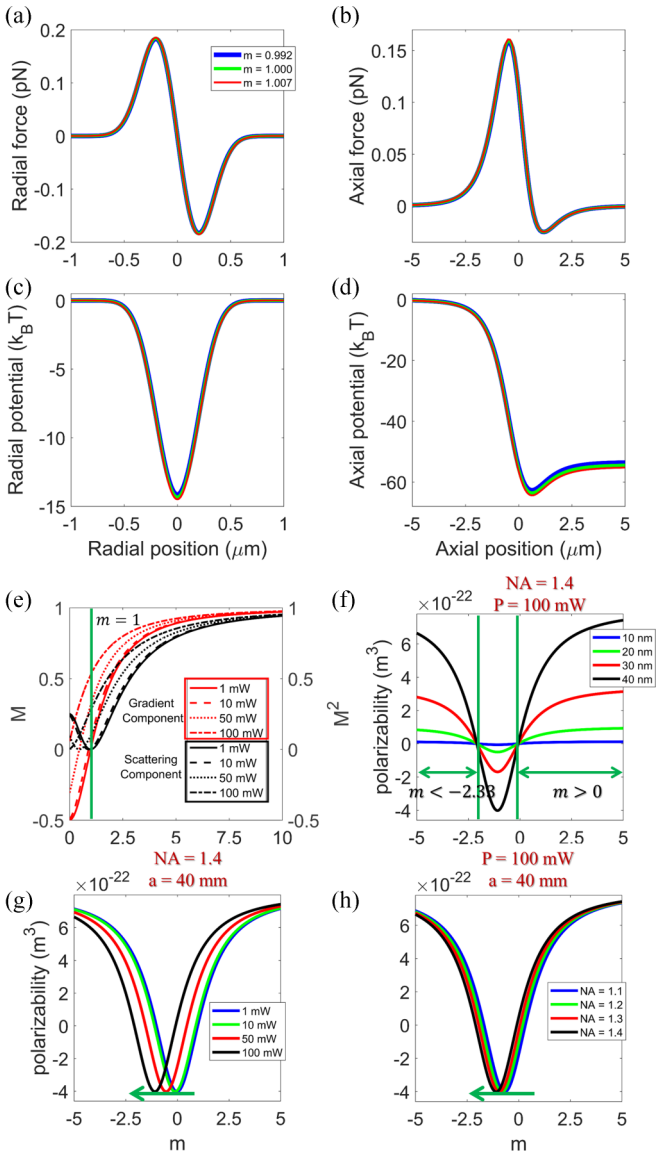

FIG. 4. Plots of trapping force along the (a) radial and (b) axial directions and the corresponding potential along the (c) radial and (d) axial directions. Plots of (e) variation of M (gradient component) and M^2 (scattering component) against relative RI, polarizability against relative RI for (f) different particle size, (g) different power, and (h) different NA under pulsed excitation.

and 4(h). With increasing power and NA, the minima of the polarizability shift toward a lower relative RI for fixed particle size. This implies that at high average power (or NA), we can trap those particles which have a significantly less RI than that of the surrounding medium, i.e., particles which cannot be trapped under CW excitation. This is one instance where one can clearly see the advantage of femtosecond pulsed excitation over CW excitation. At 100 mW average power, if the relative RI lies between −2.331 and −1.33, the particle cannot be trapped under pulsed excitation, whereas it can be trapped under CW excitation. Therefore, whether CW or pulsed excitation is more or less advantageous ultimately depends on how the relative RI is fine-tuned by optical nonlinearity. A detailed discussion of the range of relative RI, whether the particle can be trapped or not, and how it varies with power, NA, λ, and particle size is given in Secs. S2.2.1 and S2.2.2 in the SM [15].

It is interesting to note here that particles having a significantly higher RI than the surrounding medium cannot be trapped under either CW or pulsed excitations because they scatter more. In order to trap such particles, an antireflection coating on surface is required so that scattering force can be minimized [11,12]. As discussed earlier [6], that relevant quantity to determine the trapping efficiency is U_{esc} which can help in determining the optimal power for fixed a and NA. Although higher average power is required to trap smaller nanoparticles (Table S4 in the SM [15]) finding an optimal power for particle size <23 nm is very difficult because the polarizability approaches an asymptotic value at higher average power. Therefore, it is more practical to estimate an optimal particle size for a fixed laser power and NA. A detailed discussion is given in Sec. S2.2.3 in the SM [15].

IV. CONCLUSION

To summarize, using dipole approximation, we have provided a general discussion to include optical nonlinearity in laser trapping of dielectric nanoparticles. We showed how the nature of the trapping force/potential can be modulated (repulsive, intermediate, attractive, and unbound) and how particles made of low refractive index materials can be trapped by harnessing optical nonlinearity. Through this work, we envisage far-reaching applications of facile and controlled optical manipulation by tuning the nonlinear optical force.

ACKNOWLEDGMENTS

We acknowledge funding from SERB, Early Career Research Award, ECR/2016/000467, and IISER Mohali, a start-up grant and fellowship to A.D.

The authors declare no conflicts of interest.

[1] A. Ashkin, J. M. Dziedzic, J. E. Bjorkholm, and S. Chu, Observation of a single-beam gradient force optical trap for dielectric particles, Opt. Lett. **11**, 288 (1986).

[2] A. Ashkin, *Optical Trapping and Manipulation of Neutral Particles Using Lasers: A Reprint Volume with Commentaries* (World Scientific, Singapore, 2006).

[3] K. C. Neuman and S. M. Block, Optical trapping, Rev. Sci. Instrum. **75**, 2787 (2004).

[4] J. R. Moffitt, Y. R. Chemla, S. B. Smith, and C. Bustamante, Recent advances in optical tweezers, Annu. Rev. Biochem. **77**, 205 (2008).

[5] A. Ashkin, Optical trapping and manipulation of viruses and bacteria, Science **235**, 1517 (1987).

[6] A. Devi and A. K. De, Theoretical investigation on nonlinear optical effect in laser trapping of dielectric nanoparticles with ultrafast pulsed excitation, Optics Express **24**, 21485 (2016).

[7] A. Devi and A. K. De, Theoretical estimation of nonlinear optical force on dielectric spherical particles of arbitrary size under femtosecond pulsed excitation, Phys. Rev. A **96**, 023856 (2017).

[8] A. Devi and A. K. De, Simultaneous detection of two-photon fluorescence and backscatter of optical trapping of dielectric nanoparticles under femtosecond pulsed excitation, J. Nanophotonics **13**, 020501 (2019).

[9] D. Roy, D. Goswami, and A. K. De, Exploring the physics of efficient optical trapping of dielectric nanoparticles with ultrafast pulsed excitation, Appl. Opt. **54**, 7002 (2015).

[10] A. Devi and A. K. De, Nonlinear laser tweezer: Escape potential, in *Frontiers in Optics/Laser Science*, edited by B. Lee, C. Mazzali, K. Corwin, and R. Jason Jones, OSA Technical Digest (Optical Society of America, 2020), paper FTu8C.2.

[11] Y. Hu, T. A. Nieminen, N. R. Heckenberg, and H. Rubinsztein-Dunlop, Antireflection coating for improved optical trapping, J. Appl. Phys. **103**, 093119 (2008).

[12] N. Wang, X. Li, J. Chen, Z. Lin, and J. Ng, Gradient and scattering forces of anti-reflection-coated spheres in an aplanatic beam, Sci. Rep. **8**, 17423 (2018).

[13] S. Anantha Ramakrishna and T. M. Grzegorczyk, *Physics and Applications of Negative Refractive Index Materials* (CRC Press and SPIE Press, 2008).

[14] Y. Harada and T. Asakura, Radiation forces on a dielectric sphere in the Rayleigh scattering regime, Opt. Comm. **124**, 529 (1996).

[15] See Supplemental Material at http://link.aps.org/supplemental/10.1103/PhysRevResearch.2.043378 for a detail discussion of theoretical method, optical force/potential which depends on particle size, NA, refractive index, and average power under both CW and pulsed excitations.